COBEM UBERLÂNDIA 2019

ABCM Associação Brasileira de Engenharia e Ciências Mecânicas

25th ABCM International Congress of Mechanical Engineering
October 20-25, 2019, Uberlândia, MG, Brazil

COB-2019-2200
EVALUATION OF CONTROL TECHNIQUES ASSOCIATED TO AN ESTIMATOR OF THE HUMAN ELBOW MOVEMENT

Rafael da Silva Figueiredo[1]
Luciano Santos Constantin Raptopoulos[2]
Waltencir dos Santos Andrade[2]
Guilherme Amaral do Prado Campos[1,2]
Elkin Yesid Veslin Díaz[1]
Max Suell Dutra[1]
Fabrício Lopes e Silva[2]

[1]Federal University of Rio de Janeiro - Mechatronics Laboratory Jean Leon Scieszko, 2030 Horácio Macedo Av., Technology Center, Cidade Universitária, Rio de Janeiro, RJ, 21941-914, Brazil
{rafael.figueiredo, elkinveslin}@ufrj.br, max@mecanica.coppe.ufrj.br
[2]Mechatronics Research Center of the Federal Center for Technological Education Celso Suckow da Fonseca - NUPEM/CEFET-RJ, 1317 Adrianópolis Road, Nova Iguaçu, RJ, 26041-271, Brazil
{luciano.raptopoulos, waltencir.andrade, guilherme.campos, fabricio.silva, cristiano.carvalho}@cefet-rj.br

Abstract. *In the current work, performance evaluation for some control techniques is presented considering its application in an intelligent prosthesis. The challenge consists basically of an output-reference tracking problem, where the device must perform a trajectory based on a reference input signal. A dynamic model of a bench prototype was developed, as well as its movement estimator, an artificial neural network (ANN) that generates the reference trajectory based on electromyographic (EMG) signals. The chosen control methods were the computed torque and the proportional-integral-derivative (PID), both vastly used for a variety of purposes, as well as a novel control paradigm called Active Disturbance Rejection Controller (ADRC).*

Keywords: *intelligent assistive technology, control system, movement estimator, artificial neural networks, EMG signals*

1. INTRODUCTION

An assistive technology device is defined as any item, piece of equipment, or product system used to increase, maintain, or improve functional capabilities of individuals with disabilities (Alper and Raharinirina, 2006). In other words, it is any mechanism that improves the mobility of individuals with sensorial or motor limitations. In the latter case, a prosthesis is a kind of equipment that wholly or partially replaces a limb.

Prosthetics today have come a long way from primitive cosmetic prosthetics to body-powered and finally leading to the maximally advanced myoelectric prosthetics or even further advancement such as brain-computer interfacing and neuroscience (Das *et al.*, 2018). They have evolved from simple models made of iron, such as the one used by Götz von Berlichingen back in the sixteenth century (Putti, 2005), to sophisticated and lightweight mechanisms.

Myoelectric prostheses are advanced systems controlled by electromyographic (EMG) signals, which are the summation of electric potentials produced by several motor unis during muscular activation (Winter, 2009). The nervous and locomotor systems are both non-linear, being difficult to establish a relation between these two spaces. It is possible, however, to retrieve movement-related data from biological signals through machine learning, providing natural user experience. In other words, intelligent systems can map electromyographic signals into movement.

This effort is meaningless if the machines do not perform the reconstructed trajectory correctly. In this sense, the device must have not only an efficient movement estimator but also a controller with reliable reference tracking capability. Robustness is also a desirable characteristic, since external disturbances are expected to affect this kind of system. Control techniques such as PID and computed torque are often applied to prosthetics (Neogi *et al.*, 2011), in some cases adaptatively changing the control gains to improve performance (Fu *et al.*, 2019). An alternative to fulfill both design intents is the ADRC with modified plant, a variation of the relatively recent linear control paradigm.

2. METHODS

The control system for the upper limb prosthesis under development must track a reference trajectory that corresponds to the angle between the arm and the forearm. This signal is provided by an artificial neural network (ANN), which plays the role of an open-loop state observer, extracting information from electromyographic (EMG) data acquired from biceps and triceps muscle activation during flexion and extension movement in order to estimate the angular displacement of the elbow joint.

2.1 Prosthesis' dynamic model

The mechanical system's kinematic and dynamic behavior was modeled through homogeneous transform matrices. Even though only one degree-of-freedom (DOF) is studied at the current stage, the methodology proposed in this work will be extended to more DOFs in the future, corresponding to movements performed by other arm components, that for now are considered to be at rest, forming a single link with the forearm. Anthropometric data were consulted to obtain the model of an average adult human arm, that for the moment is simulated by the device in Fig. 1, developed on SolidWorks®.

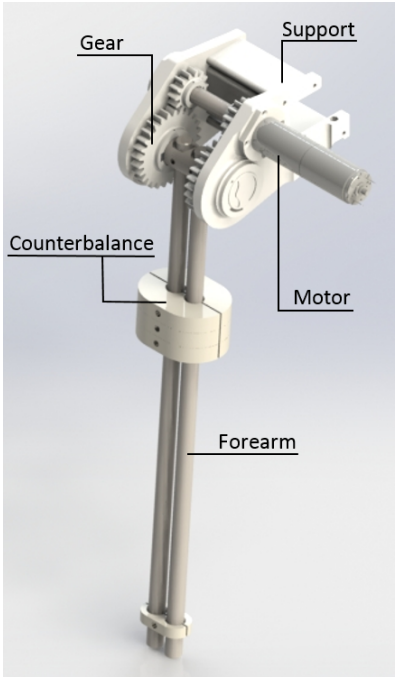

Figure 1. Prototype device developed with computer-aided design (CAD) technology.

The base of the device in Fig. 1 is fixed on the border of a workbench and accounting the shoulder condition is at rest during flexion and extension. The inertial reference system of coordinates is placed on the floor, and other two reference systems of coordinates are placed at the elbow joint and the forearm's center of mass, as indicated in the free body diagram in Fig. 2.

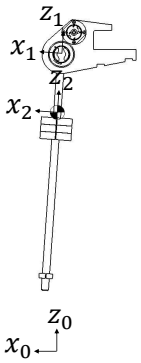

Figure 2. Free body diagram of the prosthesis with reference systems.

According to the Lagrangian formulation, the dynamic behavior is described as in Eq. (1), where $\tau(t)$ is the vector of generalized forces, while $\mathbf{q}$ and $\dot{\mathbf{q}}$ are the position vector in joint space and its first derivative with respect to time and L is called *lagrangian*, defined as the difference between the kinetic and potential energies (Niku, 2010). The lagrangian can be generically expressed as in Eq. (2) for a mechanism compound of k links.

$$\tau(t) = \frac{d}{dt}\left(\frac{\partial L}{\partial \dot{\mathbf{q}}}\right) + \frac{\partial L}{\partial \mathbf{q}} \tag{1}$$

$$L = \sum_{i=1}^{k} K_i - \sum_{i=1}^{k} U_i \tag{2}$$

Except for the lagrangian, the time variables in Eq. (1) are $k \times 1$ matrices, but as long as only the DOF corresponding to the elbow is being considered, all of them can be treated as scalars. Substitutions in Eq. (1) lead to Eq. (3), where I_{yy} is the momentum of inertia with respect to y-axis, $\ddot{q}$ is the second derivative of q with respect to time, m is the mass, g is the gravitational acceleration, and d is the distance between the articulation and the forearm's center of mass.

$$\tau = I_{yy} \cdot \ddot{q} + m \cdot g \cdot d \cdot sen(q) \tag{3}$$

A more realistic model is obtained if it is considered friction and motor inertia, resulting in Eq. (4), where n is the gearhead's reduction ratio, J_m and J_{gh} are motor and gearhead inertia respectively, and b_m and b_{gh} are dynamic friction coefficients.

$$\tau_m \cdot n = Iyy \cdot \ddot{q} + m \cdot g \cdot d \cdot sen(q) + (n^2 J_m + J_{gh}) \cdot \ddot{q} + (n^2 \cdot b_m + b_{gh}) \cdot \dot{q} \tag{4}$$

For simplicity, in the case of a higher number of degrees of freedom, Eq. 1 can be arranged to match the general notation in Eq. (5), in which $\mathbf{M}(\mathbf{q})$ is a $k \times k$ matrix called *mass matrix*, while $\mathbf{H}(\mathbf{q}, \dot{\mathbf{q}})$ and $\mathbf{G}(\mathbf{q})$ are $k \times 1$ matrices corresponding to centripetal acceleration and gravitational force, respectively.

$$\tau = \mathbf{M}(\mathbf{q})\ddot{\mathbf{q}} + \mathbf{H}(\mathbf{q}, \dot{\mathbf{q}}) + \mathbf{G}(\mathbf{q}) \tag{5}$$

2.2 Movement estimator

The element responsible for reconstructing the movement through electromyographic signals' processing is an artificial neural network. ANNs are mathematical models that reproduce the behavior of the human brain, which is a highly complex, non-linear and parallel computer (Haykin, 1998), having applications in pattern recognition, curve fitting and time series prediction, for instance. In the context of the present study, the neural network performs a *regression*; that is, it is trained to estimate the angular displacement from preprocessed EMG data.

The adopted ANN is a fully connected multilayer perceptron (MLP), consisting of twenty input nodes, two hidden neurons, and a single output neuron, as illustrated in Fig. 3. Concerning the MLP architecture, this structure is suitable to the task, as demonstrated in a previous work (Figueiredo *et al.*, 2018), and its details are summarized in Tab. 1.

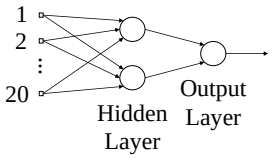

Figure 3. Artificial neural network adopted as movement estimator.

Table 1. Details about the movement estimator.

Number of hidden layers	1
Number of neurons in the hidden layer	2
Number of neurons in the output layer	1
Activation function of hidden layer's neurons	Hyperbolic Tangent Sigmoid
Activation function of output layer's neuron	Linear

The input pattern for the network in Fig. 3 is composed of ten consecutive samples of each EMG signal's envelope, while there is a single output neuron because the answer is the estimated angle.

2.3 Control techniques

Three different control techniques were selected for performance evaluation. The computed torque and the proportional-integral-derivative (PID) controller are quite simple and very present in the bibliography, while the active disturbance rejection controller (ADRC), in particular, its variation called *ADRC with modified plant*, is relatively recent when compared with the former two.

2.3.1 Computed torque

The control law for the computed torque, described in Eq. (6), comes directly from the system's dynamic model (Craig, 2005). In this equation, τ_c is the control signal (the computed torque itself), $\mathbf{K_P}$ and $\mathbf{K_V}$ are diagonal matrices of control gains, $\mathbf{e}$ and $\dot{\mathbf{e}}$ are $k \times 1$ position and velocity error matrices, respectively, and $\ddot{\mathbf{q}}_\mathbf{d}$ is the second derivative of the reference signal with respect to time. Again, for a single articulation, all these matrices can be treated as scalars.

$$\tau_c = \mathbf{M}(\mathbf{q})\left(\ddot{\mathbf{q}}_\mathbf{d} + \mathbf{K_V} \cdot \dot{\mathbf{e}} + \mathbf{K_P} \cdot \mathbf{e}\right) + \mathbf{H}(\mathbf{q}, \dot{\mathbf{q}}) + \mathbf{G}(\mathbf{q}) \tag{6}$$

The closed-loop system is illustrated in Fig. 4. In steady-state, the computed torque tends to the desired generalized forces. It means that the right side of Eqs. (5) and (6) become equal, and elimination of like terms leads to Eq. (7), which represents the error dynamics.

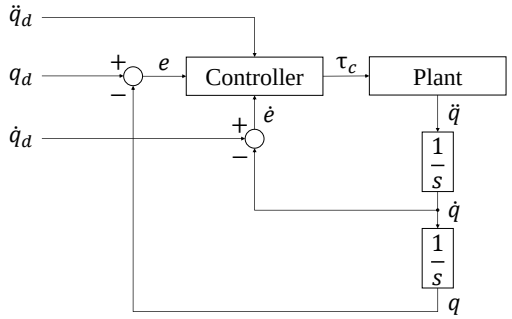

Figure 4. Block diagram of the closed-loop system with computed torque control.

$$\ddot{\mathbf{e}} + \mathbf{K_V} \cdot \dot{\mathbf{e}} + \mathbf{K_P} \cdot \mathbf{e} = 0 \tag{7}$$

Laplace Transform applied to closed-loop error dynamics results in Eq. (8). Control gains may be obtained comparing Eq. (8) to Eq. (9), the characteristic polynomial of a second order dynamic system, where ζ is called *damping ratio* and ω_n is the system's *natural frequency* (Franklin *et al.*, 2018).

$$(s^2\mathbf{I} + s\mathbf{K_V} + \mathbf{K_P})\mathbf{E}(s) = \mathbf{0} \tag{8}$$

$$p(s) = s^2 + 2\zeta\omega_n s + {\omega_n}^2 \tag{9}$$

2.3.2 Proportional-Integral-Derivative controller

The block diagram of the closed-loop system with a PID controller is shown in Fig. 5, where K_P, K_I and K_D are the control gains for the position error, its integral over time and its derivative concerning time, respectively.

Control law for the PID controller is expressed in Eq. (10), and Eq. (11) is its frequency-domain representation, from which the controller's transfer function, given in Eq. (12), is obtained.

$$u(t) = K_P \cdot e + K_I \cdot \int e\, dt + K_D \cdot \frac{\partial e}{\partial t} \tag{10}$$

$$U(s) = (K_P + K_I \cdot \frac{1}{s} + K_D \cdot s)E(s) \tag{11}$$

$$D(s) = \frac{U(s)}{E(s)} = \frac{K_D \cdot s^2 + K_P \cdot s + K_I}{s} \tag{12}$$

Naming the transfer function of the system's linearized model as $G(s)$, the closed-loop transfer funtion for unity negative feedback is written as in Eq. (13) (Nise, 2011).

$$H(s) = \frac{D(s)G(s)}{1 + D(s)G(s)} \tag{13}$$

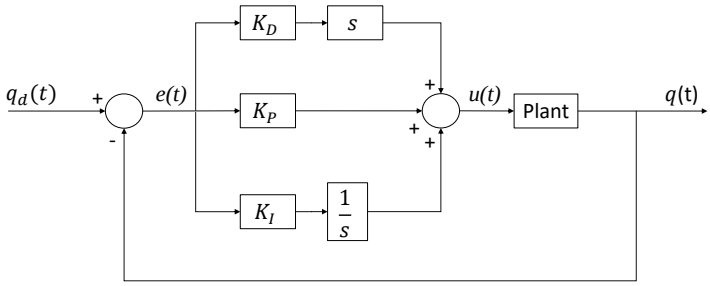

Figure 5. Block diagram of the closed-loop system with PID controller.

The control gains in Eq. (10) may be calculated comparing the denominator polynomial that emerges from Eq. (13) to the characteristic polynomial in Eq. (9). However, a linear filter in series with the closed-loop system is necessary in order to cancel the effect of closed-loop zeros on transient response.

2.3.3 ADRC with modified plant

Even though standard ADRC provides robustness to external perturbation, its reference tracking capability relies on the exact knowledge of the plant's control gain values. A state-space transformation, resulting from modification of the original system, was proposed (Correia *et al.*, 2017) to deal with this matter. This modification consists of output gain β applied to the original plant and a linear filter in parallel with both, as in the diagram in Fig. 6.

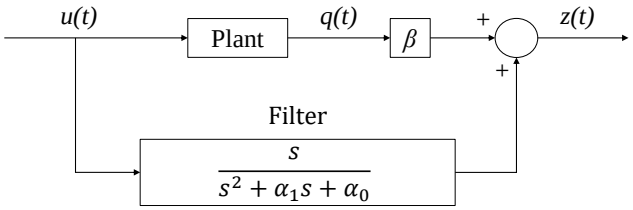

Figure 6. Diagram of the modified plant.

The stabilizing control law is given in Eq. (14), where z_d is the transformed reference signal, $\dot{z}_d$ and $\ddot{z}_d$ are its first and second derivative with respect to time and f, called *generalized perturbation*, takes into account both external perturbation and non-modeled dynamics, and may be estimated by an extended state observer. After transient response, the transformed reference is expressed as in Eq. (15).

$$\dot{u} = \dddot{z}_d + \alpha_1 \ddot{z}_d + \alpha_0 \dot{z}_d - f \tag{14}$$

$$z_d = \beta \cdot y_d \tag{15}$$

3. RESULTS

Simulations of the system and the proposed control laws were carried on MatLab®, applying a point load at hand to act as an external perturbation in the form of an object held by a user. The response provided by the studied control techniques in various flexion-extension cycles is illustrated in Figs. 7 through 12.

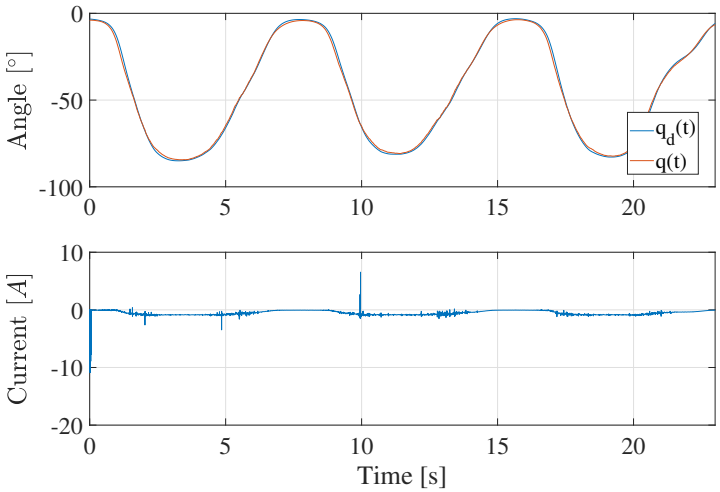

Figure 7. Closed loop system's response using computed torque control.

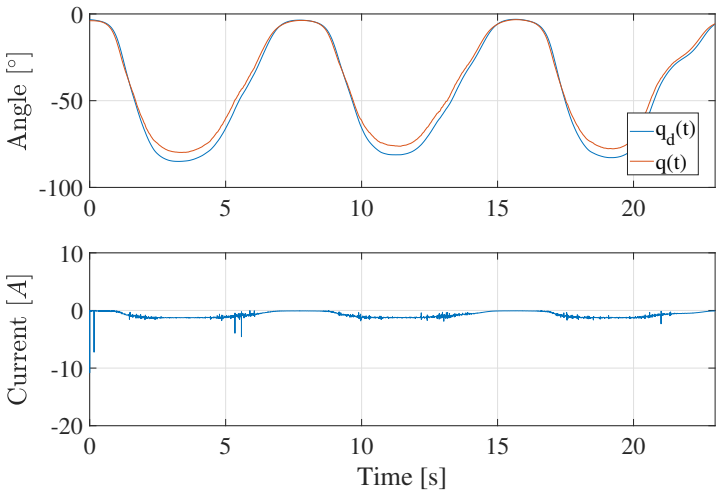

Figure 8. Closed loop system's response under effect of external disturbance using computed torque.

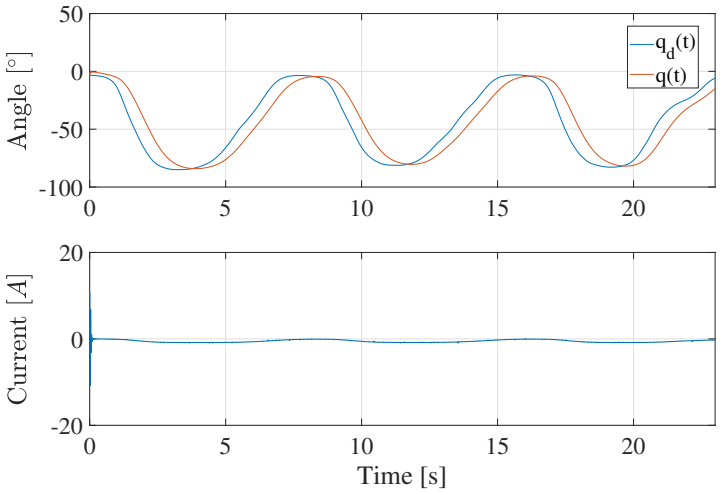

Figure 9. Closed loop system's response using a PID controller.

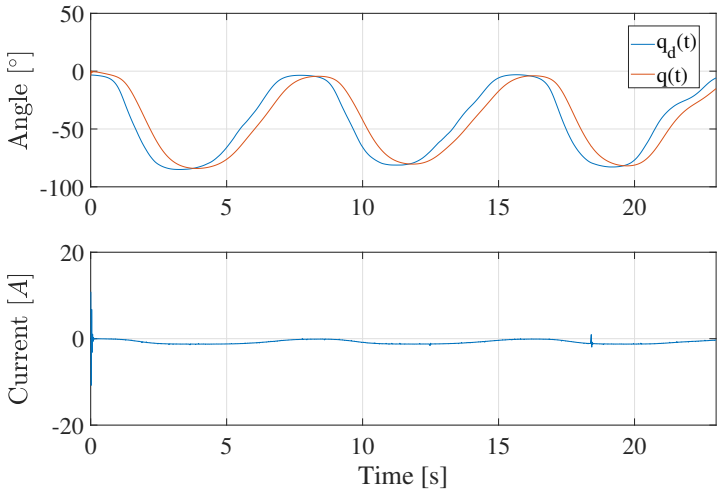

Figure 10. Closed loop system's response under effect of external disturbance using a PID controller.

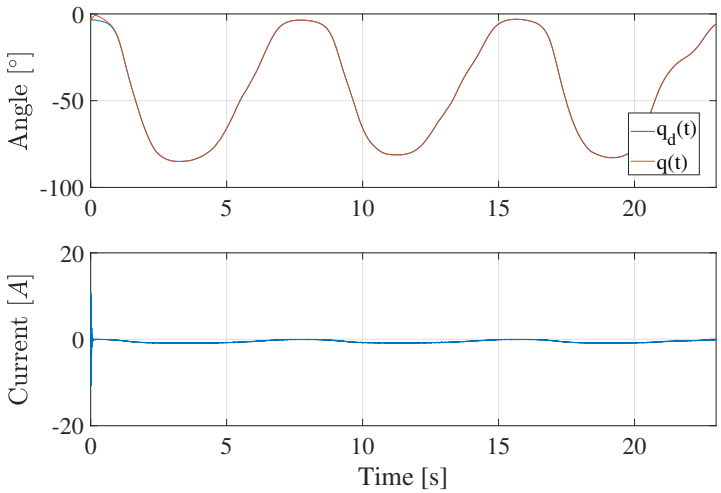

Figure 11. Closed loop system's response using ADRC with modified plant.

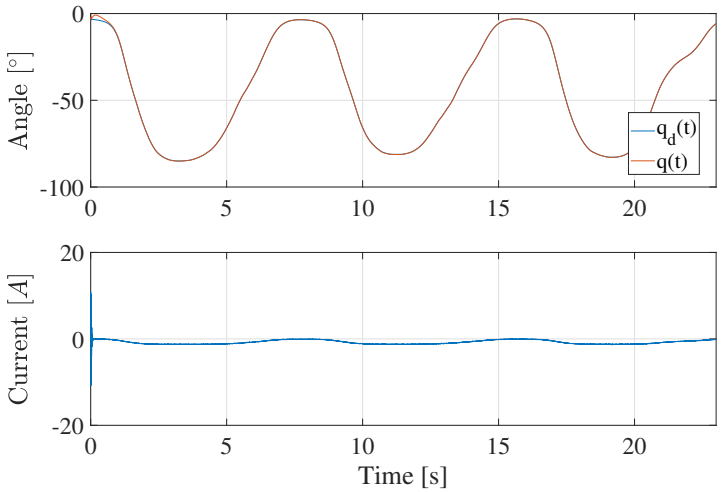

Figure 12. Closed loop system's response under effect of external disturbance using ADRC with modified plant.

From Fig. 8, it becomes clear that the computed torque is not capable of tracking the reference signal when there is a disturbance acting upon the system, this is a result of a change in the system's dynamics caused by the external perturbation, while this change is not accounted for in the controller's dynamics.

About the PID controller, it can not be said that it tracks the signal since the response is delayed about the response of the artificial neural network, as can be seen in Figs. 9 and 10.

Last, but not least, the root mean square error (RMSE) between the estimated angle and the response provided by ADRC with modified plant in Fig. 11 is approximately equal to $0.22°$. The tracking capability of this control technique, even in the presence of external disturbance, can be verified in Fig. 12. Besides, the closed-loop response presents no delay concerning the estimated movement.

4. CONCLUSIONS

Since the main design intent for the control system under development is to track the movement estimated by the artificial neural network, a proportional-integral-derivative controller is out of the question, because it tracks a delayed reference signal. Computed torque proved to be inefficient when a slight change is made in the system's dynamics. The placement of an object at the prosthesis' hand is sufficient for the control system to be unable to perform the correct movement. The ADRC with a modified plant made the prosthesis track the reference signal with $RMSE \approx 0.22°$. Results suggest that this technique could be considered for real-time applications in the field of intelligent assistive technology.

5. ACKNOWLEDGEMENTS

The present work was partially supported by CNPq, FINEP, DIPPG/CEFET-RJ, and FAPERJ.

6. REFERENCES

Correia, C.A.M., Zachi, A.R.L. and Gouvêa, J.A., 2017. "Um método de controle robusto por realimentação de saída aplicado em sistemas com parâmetros incertos". In *Proceedings of the XIII Brazilian Symposium of Intelligent Automation - SBAI*. Porto Alegre, Brazil.

Craig, J.J., 2005. *Introduction to Robotics: Mechanics and Control*. Prentice Hall, New Jersey, 3rd edition.

Das, N., Nagpal, N. and Bankura, S.S., 2018. "A review on the advancements in the field of upper limb prosthesis". *Journal of medical engineering & technology*, Vol. 42, No. 7, pp. 532–545.

Figueiredo, R.F., Carvalho, C.S., Veslin, E.Y., Silva, F.L., Campos, G.A.P., Raptopoulos, L.S.C., Bevilacqua, L., Dutra, M.S. and Andrade, W.S., 2018. "Desenvolvimento de um estimador para o movimento do cotovelo humano baseado em inteligência artificial e sinais eletromiográficos". In *Proceedings of the X National Congress of Mechanical Engineering - CONEM 2018*. Salvador, Brazil.

Franklin, G.F., Powell, J.D. and Emami-Naeini, A., 2018. *Feedback Control of Dynamic Systems*. Pearson, London, 8th edition.

Fu, Q., Pan, C. and Xu, L., 2019. "Research on the nonlinear computer torque control of the mr damper based above-knee prosthesis". In *MATEC Web of Conferences*. EDP Sciences, Vol. 267, p. 02009.

Haykin, S., 1998. *Neural Networks: A Comprehensive Foundation*. Prentice Hall, New Jersey, 2nd edition.

Neogi, B., Darbar, R., Mondal, S., Gorai, B., Ghosh, S., Das, A. and Tibarewala, D., 2011. "Study of proper tuning of prosthetic limb control system with paraplegia and fatigue condition". In *2011 Second International Conference on Emerging Applications of Information Technology*. IEEE, pp. 79–82.

Niku, S.B., 2010. *Introduction to Robotics: Analysis, Control, Applications*. John Wiley & Sons, New Jersey, 2nd edition.

Nise, N.S., 2011. *Control Systems Engineering*. John Wiley & Sons, New Jersey, 6th edition.

Putti, V., 2005. "Historical prostheses". *Journal of Hand Surgery*, Vol. 30, No. 3, pp. 310–325.

Winter, D.A., 2009. *Biomechanics and motor control of human movement*. John Wiley & Sons.

7. RESPONSIBILITY NOTICE

The authors are the only responsible for the printed material included in this paper.